AIAA JOURNAL
Vol. 45, No. 10, October 2007

Broadband Acoustic Liner Based on the Mechanism of Multiple Cavity Resonance

Xiaodong Jing,* Xiaoyu Wang,† and Xiaofeng Sun‡
Beijing University of Aeronautics and Astronautics, 100083 Beijing, People's Republic of China

DOI: 10.2514/1.27878

In this paper the mechanism of multiple cavity resonance is proposed to broaden the absorption bandwidth of an acoustic liner. The basic idea is that, when the backcavity of the liner is divided into subcavities of different size, many resonances relating to different lengths are produced so that the peaks of sound absorption become more closely distributed and take effect jointly to afford high attenuation over a large bandwidth. To study this mechanism, a cavity-resonance theory is first established to describe the coupling effect of the acoustic modes inside the subcavities and arrives at a general formula for the multiple resonance frequencies. Furthermore, a more rigorous propagation model is developed that is capable of predicting the effect of a multiresonance acoustic liner on the sound attenuation in a duct. A verification experiment is also carried out in the situation of a rectangular duct without mean flow. When compared with the experiment, the theory well predicts the resonance frequencies, while the propagation model also gives reasonably good prediction for the magnitude of the transmission loss. Both the theoretical and experimental results demonstrate the potential of the present method in improving the broadband performance of an acoustic liner.

Nomenclature

$A_{n,m}$ or A_n, $B_{n,m}$ or B_n	=	amplitudes of the upward or downward modes of the order (m, n)
a, a_c	=	width of the duct or the cavity
b	=	height of the duct
c	=	sound speed
d	=	orifice diameter of a perforated plate
$f_{n,j,m}$ or $f_{n,j}$	=	resonance frequencies of a rectangular subcavity
G_c, G_d	=	hard wall Green's function of a cavity or a rectangular duct
h	=	cavity depth
i	=	$\sqrt{-1}$
k	=	wave number in free space, ω/c
k_{mnj}	=	wave number of a cavity mode, Eq. (9b)
k_y, $k_{y,n}$	=	y-direction wave number inside a subcavity under general or resonant condition
l	=	length of a cavity or a duct segment
m, n, j	=	mode number in x, y, z directions, respectively
n_0	=	coordinate normal to the surface surrounding a region in the outward direction
p	=	total sound pressure upon the liner from outside or in a duct
p_c	=	sound pressure in the cavity
p_i, p_r, p_d	=	incident, reflected, or disturbance sound pressures in the duct
R, X	=	normalized specific acoustic resistance and reactance, respectively
$\boldsymbol{r}$, $\boldsymbol{r}_\perp$	=	coordinate vectors in 3-D space or parallel to the facing plate
S	=	area of the facing plate of the liner
t	=	time
$U_{r,m}$ or U_r	=	Fourier expansion coefficients of velocity u, Eq. (19)
u, u_d	=	acoustic particle velocity on the facing plate exposing to the liner cavity or to the duct interior
(x, y, z)	=	Cartesian coordinates
Z	=	normalized specific acoustic impedance of the facing plate
Γ_n, Σ_q	=	orthogonal values of φ_n and ϕ_q, respectively, Eq. (2c)
$\gamma_{mn}^{\pm}$, κ_{mn}	=	defining the axial wave number, Eq. (16)
δ, δ_{mn}	=	Dirac delta function or Kronecker
ε_m	=	1 for $m = 0$ or 2 for $m \geq 1$
μ_n, η_q	=	eigenvalues corresponding to φ_n and ϕ_q, respectively, Eq. (2)
ν	=	kinematic viscosity
ξ	=	coordinate perpendicular to the facing plate
ρ	=	air density
σ	=	open area ratio of a perforated plate
τ	=	thickness of a perforated plate
ϕ_q, φ_n	=	eigenfunctions of coordinate $\boldsymbol{r}_\perp$ and ξ, respectively, Eq. (2a)
ω	=	angular frequency

Superscript

(J)	=	number of a duct segment

Received 18 September 2006; revision received 12 March 2007; accepted for publication 18 May 2007.

*Professor, School of Jet Propulsion.
†Ph.D. Student, School of Jet Propulsion.
‡Professor, School of Jet Propulsion; sunxf@buaa.edu.cn (Corresponding Author).

I. Introduction

SINCE the extensive application of a perforated liner on noise control, researchers have made great efforts to pursue methods for extending the effective absorption bandwidth of this type of passive sound-absorbing structure. For various types of duct mufflers or silencers with perforated liners, it has long been a challenging problem of how to control a sound source whose frequency varies due to the change of engine operation condition or environmental conditions. A similar broadband requirement exists when an acoustic

lining is used to suppress the combustion noise. In commercial aviation, the use of the high bypass ratio engine leads to a significant reduction of the tonal noise but marked increases in the broadband component. This has given the need for a new impetus for broadband absorbers.

It is well known that the conventional perforated liners have narrow effective absorption bandwidth. The so-called locally reacting liner has a backcavity divided into cells of small cross sections, so that sound only propagates in the transverse direction inside the liner. This is the reason why the absorption peaks of this type of liners are sharp and narrow around a limited number of discrete resonance frequencies. Researchers try to extend the effective absorption bandwidth of a locally reacting liner by the use of a double- or a triple-layer structure, but this inevitably brings the penalty of increasing the size and weight of the acoustic treatment.

One way for improving the performance of an acoustic liner makes use of the basic principle that wave reflection and scattering happen at impedance discontinuities. This concept, put forth by Lansing and Zorumski [1] more that 30 years ago, has attracted much attention and evolved into many practical forms such as the more recent work about the checkerboard liner [2]. However, it is reasonable to argue about the limitation of this approach because pure wave reflection and scattering involves little absorbing effect of the total acoustic energy. Actually, the work of Watson et al. [2] shows that the optimized checkerboard liner tends to be more effective than a uniform one only at higher frequencies. And so, it is of great interest to raise the question how to activate the process of dissipating the sound energy directly by an acoustic liner.

For some time the idea of a nonlocally reacting acoustic liner has received great attention. When the partition plates are removed from the cavity of an acoustic liner, sound propagation occurs not only in the transverse direction normal to the liner facing, but also in the longitudinal direction within the backcavity. In this situation, resonances are produced in relation to two lengths that are the depth and the length of the cavity, thereby resulting in more peaks in the absorption coefficient of the acoustic liner.

It can be realized that, the more the resonances occur inside the acoustic liner, the better the possibility is for the absorption peaks to be closely spaced and jointly take effect to broaden the bandwidth of the liner. Here we propose a method to implement this idea in the way that the partition plates are purposely arranged to subdivide the backcavity into different sizes or geometry, thereby many resonances relating to different lengths occur inside the subcavities. This is what we call the mechanism of "multiple cavity resonances" and correspondingly the "multiresonance acoustic liner." In addition to the wave reflection and scattering effect, the most promising aspect of this idea is that the multiple cavity resonances can be expected to act as an effective means in enhancing sound energy dissipation of an acoustic liner.

It is crucial to establish appropriate mathematical models to gain deep insights into this mechanism. The resonance of a cavity with a perforation opening is a phenomenon of fundamental interest in acoustics. Previous attention has been paid to the situation when the wavelength is much larger than the size of the cavity, such as the lumped parameter or Helmholtz theory. As far as we know, there is a lack of simple, physically intuitive theory to treat this problem for a more general condition. In this consideration and to meet the purpose of the present study, a cavity-resonance theory is established which demonstrates that the acoustic modes inside a cavity, cutting on in different directions, are coupled to produce high fluctuating velocity through the perforation opening of the cavity. It is thus revealed the potential benefit of the multiple cavity resonance in enhancing sound reflection as well as acoustic energy dissipation of an acoustic liner. The theory arrives at a general formula for the multiple resonance frequencies covering the special case of a locally reacting acoustic liner or a conventional Helmholtz resonator.

To explore the potential of this mechanism, it is necessary to consider the interaction of a multiresonance acoustic liner with the sound wave inside a duct. However, over the past decades, theoretical models for nonlocally reacting acoustic liners were mostly set up on the unrealistic assumption that both the duct and the liner are infinitely long, such as Hughes and Dowling [3], Nayfeh et al. [4], and Rienstra [5], and therefore they are not suitable for describing the resonances in the axial direction. More recently, there is progress toward the theoretical treatment of a finite-length nonlocally reacting liner [6,7]. However, difficulty arises if a similar approach is used to investigate the proposed multiresonance acoustic liner. In the present study, an equivalent surface source and transfer matrix combined (ESS-TM) method, which was originally employed to investigate the locally reacting acoustic liners by Namba and Fukushige [8], has been developed for the present purpose. Avoiding the cumbersome process of solving the complex eigenvalues, the semi-analytical method accurately predicts the effect of a multiresonance acoustic liner on the sound propagation in a duct.

An experiment is also carried out and is compared with the theoretical prediction. Both the theory and the experiment demonstrate the effectiveness of the proposed mechanism of multiple cavity resonance in improving the performance of an acoustic liner.

II. Theoretical Modeling of the Multiple Cavity Resonances

A. General Cavity-Resonance Theory

As illustrated in Fig. 1, a multiresonance acoustic liner is different from a conventional one in that the whole backcavity is arbitrarily divided into subcavities of different sizes or geometries by acoustically hard partition plates. When a sound wave is incident on the liner, perturbation flow passes through the conductive facing plate, and high acoustic absorption occurs at certain frequencies associated with the resonances of the subcavities. In this section, a normal-mode theory is first developed to analyze this resonance phenomenon. It is assumed that the acoustic motion is harmonic with time dependence of $\exp(i\omega t)$. The analysis of the sound field inside the acoustic liner is based on the Helmholtz equation and starts from the hard-wall Green's function,

$$\begin{cases} \nabla_0^2 G_c + k^2 G_c = -\delta(\boldsymbol{r} - \boldsymbol{r}_0) \\ \frac{\partial G_c}{\partial n_0} = 0 \text{ on the cavity wall including the facing plate} \end{cases} \tag{1}$$

For a cavity whose transverse coordinate is perpendicular to the others, such as, but not necessarily limited to, a rectangular one, G_c can be expressed in the following variable-separation form:

$$G_c(\boldsymbol{r}_0;\boldsymbol{r}) = \sum_q \sum_n \frac{\Psi_{q,n}(\boldsymbol{r})\Psi_{q,n}(\boldsymbol{r}_0)}{Sh\Sigma_q \Gamma_n(\eta_q^2 + \mu_n^2 - k^2)} \tag{2a}$$

$$\Psi_{q,n}(\boldsymbol{r}) = \phi_q(\boldsymbol{r}_\perp)\varphi_n(\xi)$$

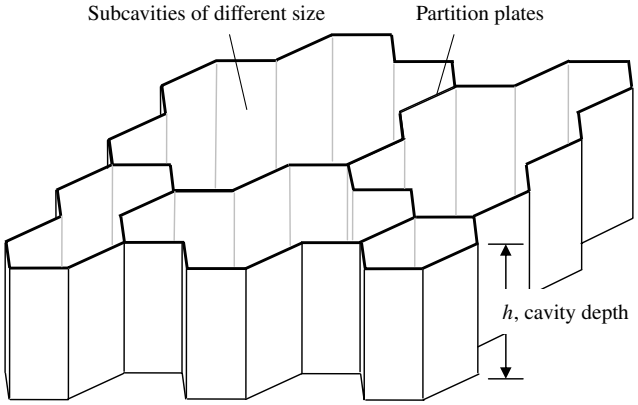

Fig. 1 An illustration of the cavity division of a multiresonance liner on the basis of, but not necessarily limited to, the conventional honeycomb structure.

$$\begin{cases} \nabla^2\Psi_{q,n} + (\eta_q^2 + \mu_n^2)\Psi_{q,n} = 0 \\ \frac{\partial\Psi_{q,n}}{\partial n_s} = 0 \text{ on the cavity wall including the facing plate} \end{cases} \tag{2b}$$

where there are orthogonal relations for the eigenfunctions:

$$\begin{aligned} \iint_S \phi_q\phi_{q'}\,\mathrm{d}S &= \begin{cases} S\Sigma_q & (q = q') \\ 0 & (q \neq q') \end{cases} \\ \int_h \varphi_n\varphi_{n'}\,\mathrm{d}\xi &= \begin{cases} h\Gamma_n & (n = n') \\ 0 & (n \neq n') \end{cases} \end{aligned} \tag{2c}$$

By use of the Green's third theorem as given by Morse and Ingard [9], the sound pressure inside the cavity is obtained,

$$p_c(r) = \iint_S G_c(\boldsymbol{r}_0;\boldsymbol{r})\frac{\partial p_c}{\partial n_0}(\boldsymbol{r}_0)\,\mathrm{d}S_0 = \rho cik\iint G_c(\boldsymbol{r}_0;\boldsymbol{r})u(\boldsymbol{r}_0)\,\mathrm{d}S_0 \tag{3}$$

The effect of the perforated facing plate is described in terms of the acoustic impedance boundary condition as

$$p - p_c(\boldsymbol{r}^-) = \rho cuZ \tag{4}$$

where the acoustic particle velocity has the positive direction pointing into the liner cavity. So, the following equation is derived from Eqs. (3) and (4):

$$\frac{p}{\rho c} = Zu + ik\iint_S G_c u\,\mathrm{d}S_0 \tag{5}$$

We further expand the sound pressure p and the acoustic particle velocity u into the series of eigenfunction ϕ_q on the facing plate, and thus defining the complex amplitudes of the acoustic modes on the facing plate as

$$\hat{p}_q = \frac{1}{S\Sigma_q}\iint p\phi_q\,\mathrm{d}S, \qquad \hat{u}_q = \frac{1}{S\Sigma_q}\iint u\phi_q\,\mathrm{d}S \tag{6}$$

With no loss of generality, the facing plate can be located at $\xi = 0$. So, substituting the Green's function (2) into Eq. (5), multiplying both sides by ϕ_q and carrying out the integration over surface S, we obtain

$$\frac{\hat{p}_q}{\rho c} = \hat{u}_q\left[Z + \frac{ik}{h}\sum_n \frac{\varphi_n^2(0)}{\Gamma_n(\eta_q^2 + \mu_n^2 - k^2)}\right] \tag{7}$$

It is evident from Eq. (7) that the absolute value of $\hat{u}_q$ or the amplitude of the velocity mode reaches its peaks when the absolute value of the term in the bracket goes to its minimums. Therefore, the multiple resonance frequencies are achieved by minimizing the following objective function:

$$E(f) = \left|Z + \frac{ik}{h}\sum_n \frac{\varphi_n^2(0)}{\Gamma_n(\eta_q^2 + \mu_n^2 - k^2)}\right| \tag{8}$$

Because of the resonance-related high bypassing perturbation velocity through the facing plate, large impedance mismatch and thus large sound reflection in the direction parallel to the facing plate occur, as well as high acoustic energy dissipation at the facing plate when there is viscous effect or nonlinear acoustic effect involved.

In the particular situation of a rectangular cavity, the hard-wall Green's function is

$$\begin{aligned} G_c(\boldsymbol{r}_0;\boldsymbol{r}) = \frac{1}{a_c hl}\sum_{m=0}^{\infty}\sum_{n=0}^{\infty}\sum_{j=0}^{\infty}\frac{\varepsilon_m\varepsilon_n\varepsilon_j}{(k_{mnj}^2 - k^2)}\cos\left(\frac{m\pi x}{a_c}\right)\cos\left(\frac{n\pi y}{h}\right) \\ \times\cos\left(\frac{j\pi z}{l}\right)\cos\left(\frac{m\pi x_0}{a_c}\right)\cos\left(\frac{n\pi y_0}{h}\right)\cos\left(\frac{j\pi z_0}{l}\right) \end{aligned} \tag{9a}$$

$$k_{mnj}^2 = \left(\frac{m\pi}{a_c}\right)^2 + \left(\frac{n\pi}{h}\right)^2 + \left(\frac{j\pi}{l}\right)^2 \tag{9b}$$

Substituting the above Green's function into Eq. (8), the objective function to be minimized for determining the resonance frequencies is written as

$$E(f) = \left|Z - \frac{ik}{k_y}\cot(k_y h)\right| \tag{10a}$$

$$k_y = \sqrt{k^2 - \left(\frac{j\pi}{l}\right)^2 - \left(\frac{m\pi}{a_c}\right)^2} \tag{10b}$$

The relation $\cot(k_y h) = (k_y/h)\sum_{n=0}^{\infty}\varepsilon_n/[k_y^2 - (n\pi/h)^2]$ has been used to derive the above equation. For each particular combination of m and j, the minimization gives a sequence of y-direction wave numbers, $k_{y,n}$, and thus the resonance frequencies of a rectangular cavity are

$$f_{n,j,m} = \frac{c}{2\pi}\sqrt{k_{y,n}^2 + \left(\frac{j\pi}{l}\right)^2 + \left(\frac{m\pi}{a_c}\right)^2} \tag{11}$$

When $m = j = 0$, Eq. (11), as expected, recovers the result for the locally reacting acoustic liner or the classical Helmholtz resonator.

When the resonance frequencies of the liner subcavities, determined by Eq. (8) for a general geometry and Eq. (11) for a rectangular one, are distributed closer to each other, a wide effective bandwidth due to the connection of the absorption peaks can be anticipated.

B. Sound Propagation Model in a Duct

The potential of a multiresonance acoustic liner is further explored to show its effect on the sound propagation in a duct. As shown in Fig. 2, the liner is located in the upper wall of an otherwise rigid, uniform rectangular duct that infinitely extends at both ends. To generate multiple resonances, the backcavity of the liner is axially divided into N subcavities of different lengths. A coordinate system is introduced in which z is along the duct axis and the origin is on the upper wall. Uniform mean flow is allowed to be present in the duct region. Although the Helmholtz equation is sufficient to describe the sound field inside the liner, the governing equation for sound propagation in the duct with the mean flow effect can be

$$\nabla^2 p - M^2\frac{\partial^2 p}{\partial z^2} - 2ikM\frac{\partial p}{\partial z} + k^2 p = 0 \tag{12}$$

In this paper, a method is developed to solve the above equation without the need of calculating the complex duct eigenvalues under a soft-wall condition. As shown in Fig. 2, the total sound pressure in a duct segment is decomposed into three components,

$$p = p_i + p_r + p_d \tag{13}$$

The incident and reflected sound pressures are supposed to be realized if every part of the duct wall is hard, while the disturbance sound pressure is that due to the existence of the acoustic liner. To facilitate the derivation, the axial coordinate z is referenced to the left end of the duct segment being considered. So, the incident and the reflected sound pressures can be written as

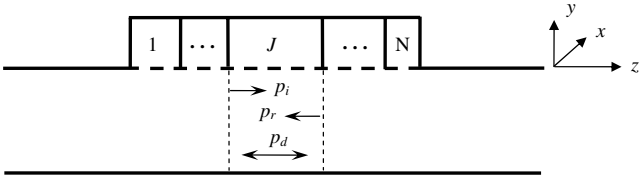

Fig. 2 Illustration of modeling the effect of a multiresonance acoustic liner on the sound propagation in a duct.

$$p_i = \sum_m \sum_n A_{n,m} \cos\left(\frac{m\pi}{a}x\right) \cos\left(\frac{n\pi}{b}y\right) \exp(i\gamma_{mn}^{+} z) \tag{14}$$

$$p_r = \sum_m \sum_n B_{n,m} \cos\left(\frac{m\pi}{a}x\right) \cos\left(\frac{n\pi}{b}y\right) \exp(i\gamma_{mn}^{-} z) \tag{15}$$

where

$$\begin{aligned} \gamma_{mn}^{\pm} &= \frac{Mk \mp \kappa_{mn}}{1-M^2} \\ \kappa_{mn} &= \sqrt{k^2 - (1-M^2)\left[\left(\frac{m\pi}{a}\right)^2 + \left(\frac{n\pi}{b}\right)^2\right]} \end{aligned} \tag{16}$$

and the branch of κ_{mn} is chosen such that $\mathrm{Re}(\kappa_{mn}) > 0$ for propagating modes or $\mathrm{Im}(\kappa_{mn}) < 0$ for decaying modes. As proposed by Namba and Fukushige [8], in terms of the normal acoustic particle velocity on the liner surface, the disturbance sound pressure can be given as

$$p_d = -i\rho c k \iint_S u_d(\boldsymbol{r}_0)\left(1 - \frac{M}{ik}\frac{\partial}{\partial z_0}\right) G_d(\boldsymbol{r}_0; \boldsymbol{r})\, \mathrm{d}S_0 \tag{17}$$

where the hard-wall joint Green's function of Eq. (12) has been introduced,

$$\begin{aligned} G_d(\boldsymbol{r}_0; \boldsymbol{r}) = &-\frac{i}{2ab} \sum_m \sum_n \frac{\varepsilon_m \varepsilon_n}{\kappa_{mn}} \cos\left(\frac{m\pi}{a}x\right) \cos\left(\frac{n\pi}{b}y\right) \\ &\times \cos\left(\frac{m\pi}{a}x_0\right) \cos\left(\frac{n\pi}{b}y_0\right) \exp[i\gamma_{mn}^{\pm}(z - z_0)] \end{aligned} \tag{18}$$

where $\gamma_{mn}^{\pm}$ has the positive sign for $z > z_0$ and the negative sign otherwise.

On the other hand, without the influence of mean flow, the sound pressure inside the liner cavity can be more directly determined from Eq. (3) by using the classical Green's function given by Eq. (9).

The impedance boundary condition, Eq. (4), is again used to connect p in the duct with p_c inside the cavity as y approaches zero from both sides of the facing plate. However, if the integral equation thus obtained is directly solved for the unknown acoustic particle velocities on the liner surface, complicated treatment has to be used to remove the singularity of the kernel functions [8]. Here a different approach is employed to overcome the singularity problem. The velocity u can be expanded into the double series of the duct eigenfunction in the x direction and the sine series in the z direction,

$$u(x, z) = \frac{1}{\rho c} \sum_m \sum_r U_{r,m} \cos\left(\frac{m\pi x}{a}\right) \sin\left(\frac{r\pi z}{l}\right) \tag{19}$$

It should be noted that the boundary condition of particle displacement continuity is assumed on the duct wall when mean flow is present, and thus the liner surface velocity exposing to the duct interior u_d is different from but related to u as

$$\begin{aligned} u_d(x, z) = \left(1 + \frac{M}{ik}\frac{\partial}{\partial z}\right) u(x, z) = \frac{1}{\rho c} \sum_m \sum_r U_{r,m} \cos\left(\frac{m\pi x}{a}\right) \\ \times \left[\sin\left(\frac{r\pi z}{l}\right) + \frac{\pi M r}{ikl} \cos\left(\frac{r\pi z}{l}\right)\right] \end{aligned} \tag{20}$$

Then, by substituting Eqs. (19) and (20) into Eqs. (3) and (17), respectively, the sound pressures, p_c and p_d, are also expressed in terms of the series expansions. Having been thus formulated, the total sound pressure in the duct p and that inside the cavity p_c must satisfy the impedance boundary condition (4); therefore we arrive at

$$\begin{aligned} &\frac{ik}{hl} \sum_s U_s \sum_n \sum_j \frac{\varepsilon_n \varepsilon_j}{k_{mnj}^2 - k^2} \cos\left(\frac{j\pi z}{l}\right) \int_0^l \sin\left(\frac{s\pi z_0}{l}\right) \cos\left(\frac{j\pi z}{l}\right) \mathrm{d}z_0 \\ &\quad + \frac{1}{2b} \sum_s U_s \sum_n \frac{\varepsilon_n}{\kappa_{mn}} \int_0^l \left(\sin\frac{s\pi z_0}{l} + \frac{s\pi M}{ikl} \cos\frac{s\pi z_0}{l}\right) \\ &\quad \times (k + M\gamma_{mn}^{\pm}) \exp[i\gamma_{mn}^{\pm}(z - z_0)] \mathrm{d}z_0 + Z \sum_s U_s \sin\left(\frac{r\pi z}{l}\right) \\ &\quad = \sum_n A_n \exp(i\gamma_{mn}^{+} z) + \sum_n B_n \exp(i\gamma_{mn}^{-} z) \end{aligned} \tag{21}$$

Note that the decoupled x modes have been suppressed when deriving the above equation, and for brevity the subscript m is dropped hereafter except where it is necessary.

As a further step, it needs to define the effective radiation impedance for the sides of the cavity and the duct, respectively, as

$$\begin{aligned} z_{rs}^{c} = &\frac{2ik}{hl^2} \sum_n \sum_j \frac{\varepsilon_n \varepsilon_j}{k_{mnj}^2 - k^2} \int_0^l \sin\left(\frac{s\pi z_0}{l}\right) \cos\left(\frac{j\pi z_0}{l}\right) \mathrm{d}z_0 \\ &\times \int_0^l \sin\left(\frac{r\pi z}{l}\right) \cos\left(\frac{j\pi z}{l}\right) \mathrm{d}z \end{aligned} \tag{22a}$$

$$\begin{aligned} z_{rs}^{d} = &\frac{1}{bl} \sum_n \frac{\varepsilon_n}{\kappa_{mn}} \int_0^l \int_0^l \sin\left(\frac{r\pi z}{l}\right) \left[\sin\left(\frac{s\pi z_0}{l}\right) + \frac{s\pi M}{ikl} \cos\left(\frac{s\pi z_0}{l}\right)\right] \\ &\times (k + M\gamma_{mn}^{\pm}) \exp[i\gamma_{mn}^{\pm}(z - z_0)] \mathrm{d}z_0 \mathrm{d}z \end{aligned} \tag{22b}$$

Then, multiplying both sides of Eq. (21) with $\sin(r\pi z/l)$ and carrying out the integration from 0 to l, the following equation is obtained:

$$\sum_s z_{rs}^{c} U_s + \sum_s z_{rs}^{d} U_s + Z U_r = \sum_n [A_n e_{rn}^{+} + B_n e_{rn}^{-}] \tag{23}$$

where

$$e_{rn}^{\pm} = \frac{2}{l} \int_0^l \sin\left(\frac{r\pi z}{l}\right) \exp(i\gamma_{mn}^{\pm} z)\, \mathrm{d}z \tag{24}$$

By supposing w_{rn}^{A} and w_{rn}^{B} are the solutions of Eq. (23) when its right-hand side is set to be e_{rn}^{+} and e_{rn}^{-}, respectively, the expansion coefficient can be given in the supposition form:

$$U_r = \sum_n A_n w_{rn}^{A} + B_n w_{rn}^{B} \tag{25}$$

Substituting Eq. (25) into Eq. (20), we obtain the normal surface velocity on the duct side. And so, the sound pressure inside a duct segment can be computed from Eqs. (14), (15), and (17), provided that the amplitudes of the incident and reflected sound pressures are known to us. Here a transfer matrix approach is used to obtain A_n and B_n. The sound fields in two neighboring duct segments, for instance, the $(J-1)$th and the Jth, are matched by the continuity of the sound pressure and its normal derivative on the interface between them, thus leading to the following linear equations:

$$\sum_v \alpha_{nv}^{+(J-1)} A_v^{(J-1)} + \beta_{nv}^{+(J-1)} B_v^{(J-1)} + \alpha_{nv}^{-(J)} A_v^{(J)} + \beta_{nv}^{-(J)} B_v^{(J)} = 0 \tag{26a}$$

$$\sum_v \tilde{\alpha}_{nv}^{+(J-1)} A_v^{(J-1)} + \tilde{\beta}_{nv}^{+(J-1)} B_v^{(J-1)} + \tilde{\alpha}_{nv}^{-(J)} A_v^{(J)} + \tilde{\beta}_{nv}^{-(J)} B_v^{(J)} = 0 \tag{26b}$$

where the matrix coefficients are derived in the Appendix. After assembling the transfer matrices for all the interfaces between the duct segments, the global matrix for the amplitudes of the incident and reflected sound pressures can be obtained as

$$\mathbf{K}\, \boldsymbol{p}_A = \boldsymbol{s} \tag{27}$$

where

$$\mathbf{K} = \begin{bmatrix} \begin{bmatrix} \delta_{nv} & \alpha_{nv}^{-(1)} & \beta_{nv}^{-(1)} \\ \gamma_{mn}^{-}\delta_{nv} & \tilde{\alpha}_{nv}^{-(1)} & \tilde{\beta}_{nv}^{-(1)} \end{bmatrix} & & & & 0 \\ & \begin{bmatrix} \alpha_{nv}^{+(2)} & \beta_{nv}^{+(2)} \\ \tilde{\alpha}_{nv}^{+(2)} & \tilde{\beta}_{nv}^{+(2)} \end{bmatrix} & \alpha_{nv}^{-(2)} & \beta_{nv}^{-(2)} & \\ & & \tilde{\alpha}_{nv}^{-(2)} & \tilde{\beta}_{nv}^{-(2)} & 0 \\ 0 & & \cdots & & \\ & 0 & & \begin{bmatrix} \alpha_{nv}^{+(N)} & \beta_{nv}^{+(N)} \\ \tilde{\alpha}_{nv}^{+(N)} & \tilde{\beta}_{nv}^{+(N)} \end{bmatrix} & \begin{matrix} -\delta_{nv} \\ -\gamma_{mn}^{+}\delta_{nv} \end{matrix} \end{bmatrix}$$

$$\boldsymbol{p}_A = [B_v^{(0)}, A_v^{(1)}, B_v^{(1)}, \ldots, A_v^{(N+1)}]^T$$
$$\boldsymbol{s} = [-A_n^{(0)}, -\gamma_{mn}^{+}A_n^{(0)}, 0, \ldots, 0]^T$$

In the above equations, $A_n^{(0)}$ are the amplitudes of the incident sound wave in the hard-wall duct section, and $A_n^{(N+1)}$ are those of the transmitted sound wave. After determining the sound pressure in the duct, we can compute the transmission loss (TL) and the absorption coefficient that, according to [6], are defined as the ratio of transmitted acoustic energy to the incident, and the net absorbed sound energy divided by the energy incident on the liner section, respectively.

C. Acoustic Impedance of Perforated Plate

In the present work a facing plate of perforated type is used. On the basis of Maa's [10] approximate formula and Melling's [11] method of adding the end corrections, we are able to set up an impedance model for a perforated plate as follows:

$$\begin{aligned} R(\omega) &= \frac{32\nu(\tau + d)}{\sigma c d^2}\sqrt{1 + \frac{q^2}{32}} \\ X(\omega) &= \frac{k\tau}{\sigma}\left[\left(1 + 1\Big/\sqrt{9 + \frac{q^2}{2}}\right) + 0.85\frac{d}{\tau}\right] \end{aligned} \tag{28}$$

where $q = (d/2)\sqrt{\omega/\nu}$. The above equation shows that both resistance and reactance are functions of frequency but the resistance part only shows weak dependency.

The collaboration of the impedance model (28) with the cavity-resonance theory or the duct propagation model leads to the complete formulation of the physical problem being considered.

III. Experiment

The present experimental setup is shown in Fig. 3. The multiresonance acoustic liner under test is mounted in the middle of a straight, rectangular waveguide of 100 mm both in width and height. The liner consists of a perforated plate and a backcavity that has a 100 mm × 100 mm cross section and a total length of 518 mm. Two perforated plates are tested whose geometrical parameters are given in Table 1.

There are nine pairs of slots, uniformly spaced at 50 mm, in the inner sidewall of the liner cavity, so that 2 mm-thick partition plates can be inserted into or removed from the cavity to form subcavities of different lengths. For instance, as in Fig. 3, the whole cavity has been divided into three subcavities whose lengths are 102, 154, and 258 mm, respectively. For simplicity, in the following context the length ratio of the subcavities is round up to integer values, thus it is 2:3:5 in this case. To prevent air leakage, sealing has been done along the slots and edges of the partition plates.

A sound source consisting of four loudspeakers is connected to one end of the waveguide. At the other end of the waveguide, a sound-absorbing wedge inside the duct provides an anechoic termination whose absorption coefficient is over 0.96 above 150 Hz. The measurements are carried out below 1500 Hz to make sure there is only plane wave propagating in the hard-wall section of the waveguide. A multitone source excitation is used in the experiment which is composed of harmonic components with a small frequency interval of 10 Hz within the range from 50 to 1500 Hz. Three B&K 1/2 in. microphones are flush mounted in the wall of the waveguide. The first two microphones form a pair separated by 100 mm in front of the entrance of the liner section, and the third one is behind the exit of the liner section. From the measured sound pressures of the microphone pair, the sound wave in the hard-wall duct segment between the source and the test liner can be decomposed into the incident and reflected waves using the two-microphone technique developed by Chung and Blaser [12]. The transmitted sound wave through the liner section is measured by the third microphone. In the experiment, the sound pressure level (SPL) of the incident sound wave is kept around 80 dB.

IV. Results and Discussion

A. Validation of the ESS-TM Method

For validation purposes, a comparison is first made between the present ESS-TM model and the theory of Eldredge and Dowling [6] for the duct liner configuration in the reference. By use of the eigenfunctions in a cylindrical coordinate system, it is straightforward to modify the present model for the situation of a circular duct. The impedance model of a perforated plate given by Eq. (28) is also modified to include the bias flow effect as that in [6]. Excellent agreement is seen between the two theoretical methods in Fig. 4.

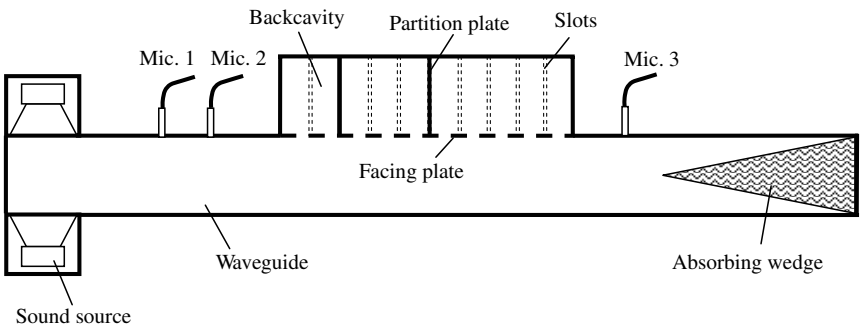

Fig. 3 The schematic of the experimental setup.

Table 1 Geometrical parameters of the test perforated plates

No.	d, mm	τ, mm	σ, %
1	3.0	1.1	10.0
2	1.0	0.8	2.0

Furthermore, we compare the ESS-TM model with the experiment for the simple case of an expansion chamber without perforated facing plate, as shown in Fig. 5. The agreement between the measured transmission loss and the theoretical prediction is satisfactory. The above comparisons have lent us credence further to apply the present semi-analytical method to the investigation of a multiresonance acoustic liner.

B. Discussion of Theoretical and Experimental Results

A perforated plate together with a backcavity forms an acoustic liner. When the cavity is divided into 10 subcavities, the transmission loss of the acoustic liner is given as a function of frequency in Fig. 6. There is a single peak on the curve of the transmission loss, and this is evident because the geometry of the subcavities only allows the transverse resonance to occur. The peak frequency is near the theoretical value of 641 Hz, given by the special case of Eq. (11) when $m = j = 0$. Although the TL peak is up to about 50 dB, the acoustic liner has a very narrow effective bandwidth, which is typically regarded as the locally reacting characteristic.

When all the partition plates are removed from the cavity, more resonance peaks appear on the transmission loss curve, as shown in Fig. 7. There is even a flat and high TL band from about 900 to 1100 Hz with the values being averaged over 20 dB; thus the nonlocally reacting effect is demonstrated. According to the theory in Sec. II.A, the TL peaks are related to the multiple resonances due to the couple (coupling) of the modes cutting on in different directions inside the cavity, and the resonance frequencies can be estimated by Eq. (11). Such results are presented and denoted by arrows in Fig. 7, showing generally good agreement with those of the experiment and the ESS-TM model. Being of zero order and decoupled from the other two, the x mode has been omitted in the analysis and the corresponding index has been dropped from the variable $f_{n,j}$ for the theoretical resonance frequencies. It can be seen that, for a nonlocally reacting acoustic liner, the first transverse resonance is not necessarily dominant; it only produces a small peak at about 640 Hz in this case. The high TL peaks are due to the (1, 2) and (1, 3) resonances that originate from the coupling of the first y mode with the second and the third modes in the z direction, respectively. In this case, the transverse mode and the axial modes have shown an unexpectedly strong coupling effect.

We further consider the situation of a multiresonance acoustic liner inside whose cavity partition plates are purposely arranged. Figure 8 shows the case where the liner cavity is subdivided into two at different length ratios. As expected, several peaks occur on the curve of the transmission loss, and their positions have been considerably changed in comparison with the nonpartition-plate case of Fig. 7. When the length ratio is 3:7 as shown in Fig. 8a, the first transverse resonance peak emerges as the dominant one, and next to it toward high frequency are (1, 1) and (1, 2) resonance peaks at correspondingly 830 and 1080 Hz (measured values), associated with the second subcavity. The (1, 1) resonance peak due to the first subcavity has a higher frequency of 1250 Hz since the cavity has a smaller length. Unfortunately, the (1, 1) resonance peak at 830 Hz is quite a modest one with a value of just above 10 dB. So, although the transmission loss curve is overall raised by the connection of the peaks, the result is not as satisfactory as expected. However, when the length ratio of the subcavities is adjusted to 2:8, a very different result is obtained as shown in Fig. 8b. In this case, the first subcavity has a length equal to the duct width, so it only generates the transverse resonance that results in the (1, 0) TL peak at about 640 Hz, while the second subcavity produces high TL peaks by (1, 1) and (1, 2) resonances at about 790 and 940 Hz, respectively. We can see from the figure that, as a result of the joint effect of the three peaks, a high TL band appears from 600 to 1000 Hz with the average value being over 15 dB. Compared with the nonpartition-plate case in Fig. 7, the TL peaks are also moved toward the low frequency although the total length of the acoustic liner is unchanged.

A perforated plate of different geometrical parameters is also used in the study, and the results are presented in Fig. 9. When the length ratio of the subcavities is 4:6, it can be seen from the transmission loss

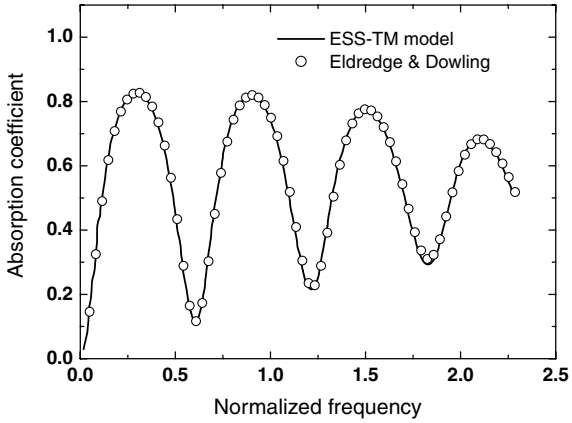

Fig. 4 Comparison between the present model and the theory of Eldredge and Dowling [6] for the case of Fig. 5 in the reference.

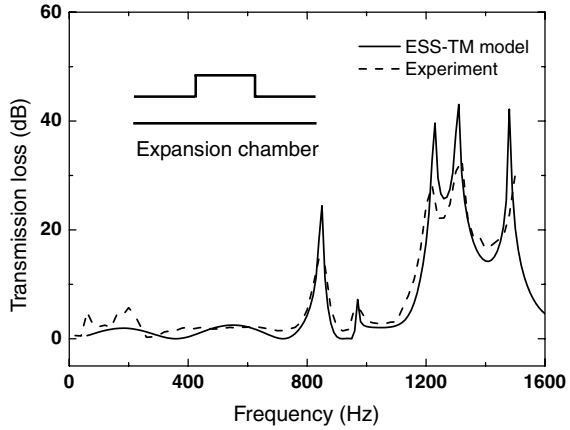

Fig. 5 The transmission loss as a function of frequency for the expansion chamber without perforated facing plate.

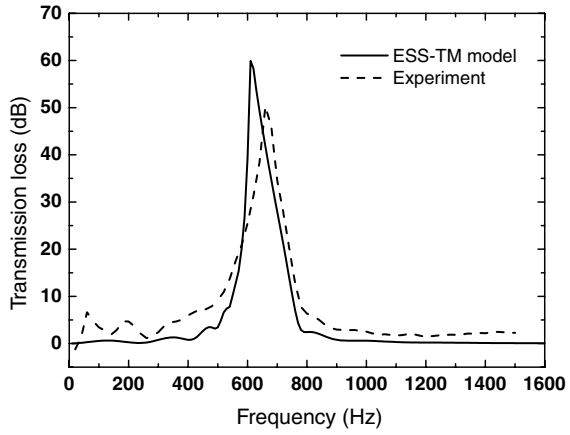

Fig. 6 The transmission loss as a function of frequency for the acoustic liner consisted of perforated plate No. 1 and a cavity divided into 10 identical cells of 50 mm in length.

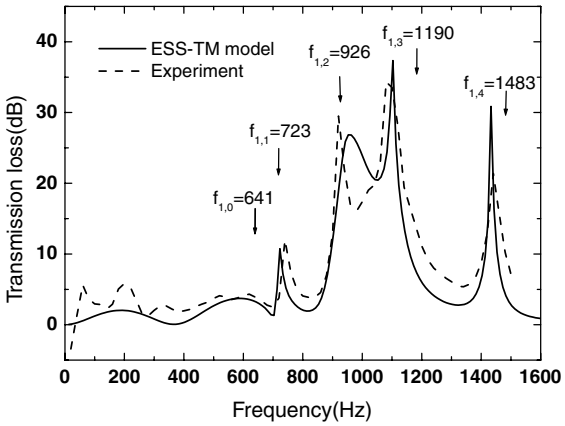

Fig. 7 The transmission loss as a function of frequency for the acoustic liner consisted of perforate plate No. 1 and a nonpartitioned cavity, and $f_{n,j}$ is the resonance frequency given by Eq. (11) when $m = 0$.

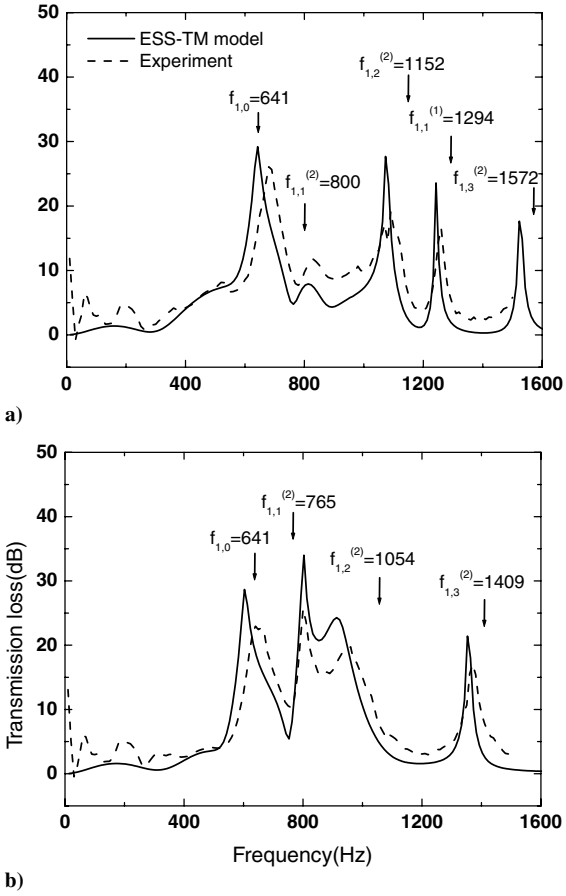

Fig. 8 The transmission loss as a function of frequency for the multiresonance liner consisted of perforated plate No. 1 and a subdivided cavity at the length ratio of a) 3:7 and b) 2:8, and $f_{n,j}$ is the resonance frequency given by Eq. (11) with its superscript denoting the number of the subcavities.

curve that the first transverse resonance peak connects with the (1, 1) resonance peak of the second subcavity to broaden the bandwidth of the acoustic liner.

In Figs. 7–9, the predictions of the ESS-TM model are in generally good agreement with the experiment for an acoustic liner, but show larger deviation compared with the case of a simple expansion chamber without a perforated plate. An error analysis indicates that the variation in the impedance of a perforated plate can be a major influential factor to the computed transmission loss. However, due to manufacturer error and other practical complexities, it is very

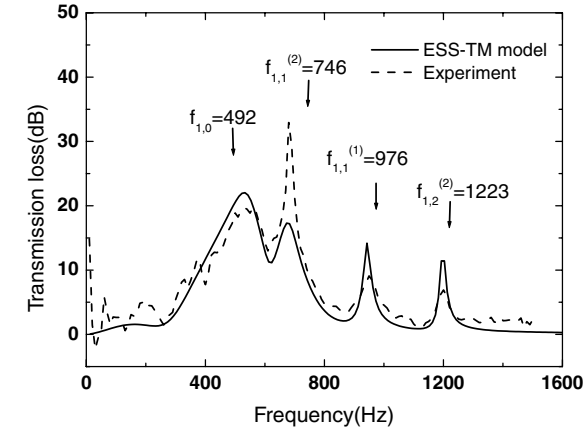

Fig. 9 Presentation similar to Fig. 8 but for an acoustic liner consisting of perforated plate No. 2 and a subdivided cavity at the length ratio of 4:6.

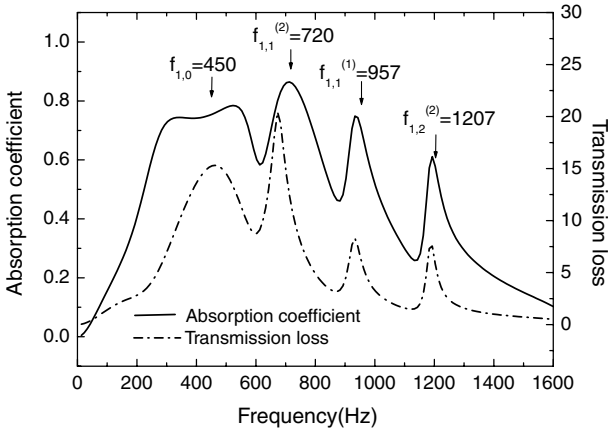

Fig. 10 The absorption coefficient and the transmission loss for a multiresonance liner consisting of a subdivided cavity at the length ratio of 4:6 and a resistive microperforated plate whose parameters are $d = 0.5$ mm, $\tau = 1.0$ mm, and $\sigma = 1.5\%$.

difficult to accurately predict the impedance of a perforated plate by a theoretical model such as Eq. (28). Besides, we cannot completely rule out the possibility of nonlinear effects that probably happen at comparatively low sound pressure levels when the resonances occur. One should also note that it is perhaps the best but still an approximate treatment to smear the discrete character of a perforated plate into a continuous impedance representation.

The perforated plates used in the experiment, with orifices as large as one to several millimeters, have small acoustic resistance of $0.1–0.2\rho c$ within the range of test frequencies. With little dissipation effect, the transmission loss in Figs. 7–9 is mainly due to the reflection of the incident sound wave back toward the source end. However, as we know, resonance usually acts as an effective means to enhance acoustic energy dissipation. This mechanism is theoretically investigated in Fig. 10 when large acoustic resistance is provided by a microperforated plate with orifices as small as 0.5 mm. We can see that a high absorption coefficient of about 0.8 is reached at the first three resonance peaks, that is, the transverse one and the other two related to the first axial modes of the two subcavities. In Fig. 10, as for the peak frequencies of the absorption coefficient, Eq. (11) and the ESS-TM model are in excellent agreement. Except for small deviations, each peak frequency of the absorption coefficient is matched fairly well with that of the transmission loss. This clearly demonstrates that, under the multiple resonance condition, large fluctuating velocity through the perforated plate is produced, thus resulting in high sound reflection as well as high acoustic energy absorption at the acoustic liner, as analyzed by the cavity-resonance theory. Microperforated plates are difficult to manufacture and to maintain in a dusty environment. To increase the

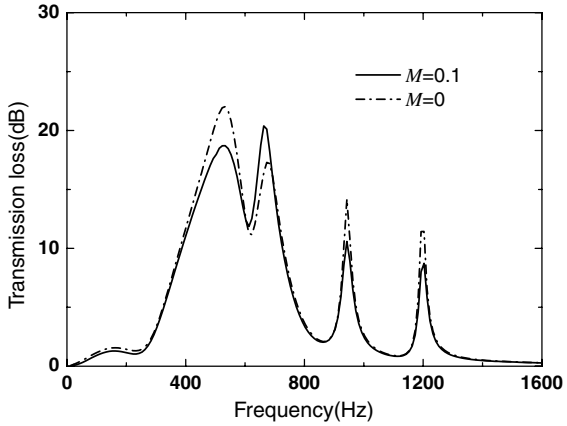

Fig. 11 The influence of mean flow on the transmission loss of a multiresonance acoustic liner, simulated by the ESS-TM model.

acoustic resistance, an alternative way is by the bias flow effect [6,7] or the acoustic nonlinearity at high SPL that occurs in many practical situations.

The mean flow in the duct is another practical influential factor. When the Mach number of the mean flow is 0.1, the simulation result of the ESS-TM model is shown in Fig. 11, in contrast to the corresponding nonflow case of Fig. 9. As we can see, the first dominant absorption peak is reduced by about 3 dB, whereas the second one, which is due to the couple (coupling) of the transverse and longitudinal modes, is increased by nearly the same amount. However, the resonance frequency of each absorption peak is only slightly changed by the presence of mean flow. This is quite an expected result because the subcavities that create the multiple resonances are free from the mean flow influence.

This paper considers only a rectangular acoustic liner with axially divided backcavity. For a circular acoustic liner, it is also attractive to circumferentially divide the backcavity for creating the multiple resonances. If the liner cavity is nonuniformly partitioned in both axial and circumferential directions, it is suggested that a new geometrical parameter, that is, the size of the subcavities, takes a role in the liner design, in addition to the conventional four parameters: the cavity depth, the orifice diameter, the plate thickness, and the open area ratio. Therefore, this implies that an optimization method is necessary for the best "tuning" of a multiresonance acoustic liner in the design process.

V. Conclusions

This paper proposes to broaden the effective bandwidth of an acoustic liner with the multiple cavity resonances produced by dividing the liner cavity into subcavities of judiciously selected length or geometry. This mechanism has been studied by 1) a simple but physically intuitive cavity-resonance theory, and 2) a more rigorous ESS-TM (effective surface source and transfer matrix combined) propagation model that predicts the effect of a multiresonance acoustic liner on the sound propagation in a duct. The two theoretical methods are compared with experiment with good agreement. The analysis based on the theoretical and experimental results arrives at the following understanding of the multiple cavity-resonance mechanism:

1) By subdividing the backcavity, more sound absorption peaks occur due to the couple (coupling) of the acoustic modes in different directions inside the subcavities and the multiple resonances thus produced, and the peak frequencies have been considerably changed in comparison with the case of nonpartitioned cavity.

2) The coupling effect between the transverse modes and the axial modes can be very strong so that the first transverse resonance is not necessarily as dominant as it usually is for a locally reacting acoustic liner.

3) There is a good possibility that the bandwidth of the high transmission loss can be markedly broadened by the connection of the multiple resonance peaks, and moreover this can happen at comparatively low frequencies.

4) Multiple cavity resonance not only produces sound reflection as with the previous methods by means of scattering or impedance discontinuity, but also provides an effective means to enhance acoustic energy dissipation at an acoustic liner.

The potential benefits of this method are demonstrated for improving the broadband and low-frequency performance of an acoustic liner without the need to increase the length or depth of the liner cavity. Although promising, the proposed methodology needs further study to be fully explored.

Appendix: Derivation of Elements in the Transfer Matrix

By the use of u_d in the expansion form (20) with the coefficients being given by Eq. (25), the disturbance sound pressure of Eq. (17) can be written as follows for the downward and upward directions, respectively:

$$p_d = -\sum_n \cos\left(\frac{n\pi y}{b}\right)\frac{(k+M\gamma_{mn}^-)}{\kappa_{mn}}\exp(i\gamma_{mn}^- z) \times \sum_v (a_{nv}^- A_v + b_{nv}^- B_v) \quad \text{for } z<0 \tag{A1a}$$

$$p_d = -\sum_n \cos\left(\frac{n\pi y}{b}\right)\frac{(k+M\gamma_{mn}^+)}{\kappa_{mn}}\exp(i\gamma_{mn}^+ z) \times \sum_v (a_{nv}^+ A_v + b_{nv}^+ B_v) \quad \text{for } z>l \tag{A1b}$$

where

$$a_{nv}^{\pm} = \sum_r w_{rv}^A f_{rn}^{\pm}, \qquad b_{nv}^{\pm} = \sum_r w_{rv}^B f_{rn}^{\pm} \tag{A2}$$

and letting

$$f_{rn}^{\pm} = \frac{\varepsilon_n}{2b}\int_0^l \left[\sin\left(\frac{r\pi z}{l}\right) + \frac{\pi M r}{ikl}\cos\left(\frac{r\pi z}{l}\right)\right]\exp(-i\gamma_{mn}^{\pm} z)\,\mathrm{d}z \tag{A3}$$

It should be mentioned that both the above integration and those for $e_{rn}^{\pm}$ and the effective radiation impedances, z_{rs}^d and z_{rs}^c, in Sec. II.B can be analytically carried out, but for conciseness these results are omitted in this paper. Now, it is straightforward to compute the total sound pressure p and its normal derivatives at the left and right ends of the duct segment where $z = 0^-$ and $z = l^+$, respectively. Finally, the application of the continuity condition of p and $\partial p/\partial z$ on the interface between the Jth and the $(J-1)$th segment gives linear equations (26) whose coefficient elements are given as follows:

$$\alpha_{nv}^{+(J)} = \lambda_n^{+(J)}\left(\delta_{nv} - \frac{k+M\gamma_{mn}^+}{\kappa_{mn}}a_{nv}^{+(J)}\right)$$

$$\alpha_{nv}^{-(J)} = -\delta_{nv} + \frac{k+M\gamma_{mn}^-}{\kappa_{mn}}a_{nv}^{-(J)}$$

$$\beta_{nv}^{+(J)} = \lambda_n^{-(J)}\delta_{nv} - \frac{\lambda_n^{+(J)}(k+M\gamma_{mn}^+)}{\kappa_{mn}}b_{nv}^{+(J)}$$

$$\beta_{nv}^{-(J)} = -\delta_{nv} + \frac{k+M\gamma_{mn}^-}{\kappa_{mn}}b_{nv}^{-(J)}$$

and

$$\tilde{\alpha}_{nv}^{+(J)} = \gamma_{mn}^+\alpha_{nv}^{+(J)}, \qquad \tilde{\alpha}_{nv}^{-(J)} = \gamma_{mn}^-\alpha_{nv}^{-(J)} + (\gamma_{mn}^- - \gamma_{mn}^+)\delta_{nv}$$

$$\tilde{\beta}_{nv}^{+(J)} = \gamma_{mn}^+\beta_{nv}^{+(J)} + (\gamma_{mn}^- - \gamma_{mn}^+)\lambda_n^{-(J)}\delta_{nv}, \qquad \tilde{\beta}_{nv}^{-(J)} = \gamma_{mn}^-\beta_{nv}^{-(J)}$$

where $\lambda_n^{\pm} = \exp(i\gamma_{mn}^{\pm} l)$.

Acknowledgments

The sponsorship of the National Natural Science Foundation of China (No. 50136010) and the Fok Ying Tung Educational Foundation (No. 91052) is gratefully acknowledged.

References

[1] Lansing, D. L., and Zorumski, W. E., "Effect of Wall Admittance Changes on Duct Transmission and Radiation of Sound," *Journal of Sound and Vibration*, Vol. 27, No. 1, 1973, pp. 85–100.

[2] Watson, W. R., Robinson, J. H., Jones, M. G., and Parrott, T. L., "Computational Study of Optimum and Off-Design Performance of Checkerboard Liners," AIAA Paper 2004-3030, 2004.

[3] Hughes I. J., and Dowling, A. P., "The Absorption of Sound by Perforated Linings," *Journal of Fluid Mechanics*, Vol. 218, Sept. 1990, pp. 299–335.

[4] Nayfeh, A. H., Kaiser, J. E., and Telionis, D. P., "Acoustics of Aircraft Engine-Duct Systems," *AIAA Journal*, Vol. 13, Feb. 1975, pp. 130–153.

[5] Rienstra, S. W., "Contributions to the Theory of Sound Propagation in Ducts with Bulk-Reacting Lining," *Journal of the Acoustical Society of America*, Vol. 77, No. 5, 1985, pp. 1681–1685.

[6] Eldredge, J. D., and Dowling, A. P., "The Absorption of Axial Acoustic Waves by a Perforated Liner with Bias Flow," *Journal of Fluid Mechanics*, Vol. 485, June 2003, pp. 307–335.

[7] Eldredge, J. D., "On the Interaction of Higher Duct Modes with a Perforated Liner System with Bias Flow," *Journal of Fluid Mechanics*, Vol. 510, July 2004, pp. 303–331.

[8] Namba, M., and Fukushige, K., "Application of the Equivalent Surface Source Method to the Acoustics of Duct Systems with Non-Uniform Wall Impedance," *Journal of Sound and Vibration*, Vol. 73, No. 1, 1980, pp. 125–146.

[9] Morse, P., and Ingard, K., *Theoretical Acoustics*, McGraw–Hill, New York, 1968, p. 321.

[10] Maa, D-Y., "Potential of Microperforated Panel Absorber," *Journal of the Acoustical Society of America*, Vol. 104, No. 5, 1998, pp. 2861–2866.

[11] Melling, T. H., "The Acoustic Impedance of Perforates at Medium and High Sound Pressure Levels," *Journal of Sound and Vibration*, Vol. 29, No. 1, 1973, pp. 1–65.

[12] Chung, J. Y., and Blaser, D. A., "Transfer Function Method of Measuring In-Duct Acoustic Properties: 1. Theory and 2. Experiment," *Journal of the Acoustical Society of America*, Vol. 68, No. 3, 1980, pp. 907–921.

C. Bailly
Associate Editor